Effect of Growth Condition on Mechanical Properties of Zirconium Carbonitride Absorber-Based Spectrally Selective Coatings

B. Usmani, V. Vijay, R. Chhibber and Ambesh Dixit

Abstract Zirconium carbonitride (ZrC–ZrN) absorber layer has been optimized for the maximum absorptivity $\alpha \sim 0.9$ in ZrO_x/ZrC–ZrN/Zr reflector–absorber tandem structures on stainless steel (SS) and aluminum (Al) substrates, using reactive DC/RF magnetron sputtering process and varying reactive nitrogen during the deposition. The mechanical properties such as hardness and Young's modulus values increase from ~19.63 to ~38.53 GPa and ~36.39 to ~58.67 GPa, respectively, with increasing nitrogen flow rate during ZrC–ZrN absorber layer deposition on SS substrate. These values also increase with increasing load up to a critical limit and saturates thereafter with further increase in load values. The films with moderate hardness and Young's modulus exhibit enhanced solar thermal performance ($\alpha \sim 0.9$) against films with lower and higher values of these mechanical properties, suggesting optimal nitrogen concentration for desired solar thermal performance.

Keywords Spectrally selective coatings · Nanoindentation · Young's modulus · Hardness · Absorptance · Emittance

B. Usmani · A. Dixit (✉)
Department of Physics and Center for Solar Energy,
Indian Institute of Technology Jodhpur, Jodhpur 342011, Rajasthan, India
e-mail: ambesh@iitj.ac.in

V. Vijay
Department of Mathematics, Indian Institute of Technology Jodhpur, Jodhpur 342011, Rajasthan, India

R. Chhibber
Department of Mechanical Engineering, Indian Institute of Technology Jodhpur, Jodhpur 342011, Rajasthan, India

L. Chandra and A. Dixit (eds.), *Concentrated Solar Thermal Energy Technologies*,
Springer Proceedings in Energy, https://doi.org/10.1007/978-981-10-4576-9_13

1 Introduction

There are continuous efforts to design and develop spectrally selective coating, which may withstand high-temperature and harsh environmental conditions. The structural, thermo-physical, mechanical, and corrosion stabilities are essential for the longevity of solar thermal systems. Recently, zirconium carbonitride based spectrally selective coatings have shown promise because of their high-temperature stability and moderate corrosion resistance [1–3]. In addition, the mechanical stability of these spectrally selective coating is indispensable for the long-term stability of the solar thermal properties and thus the system performance. The mechanical properties such as hardness and Young's modulus of the spectrally selective absorbers are important to optimize for optimal solar thermal performance. Therefore, there is a need to understand the correlation of mechanical properties with synthesis conditions, which may be used to design the optimal coating structures with enhanced solar thermal performance in conjunction with their mechanical stability.

Atomic Force Microscopy (AFM) is used to measure the repulsive and attractive forces between a given sample surface and an AFM tip, for mapping the topography of the material at nanometer resolution. Further, in contact mode, AFM has been employed to measure the mechanical properties such as hardness and Young's modulus of the thin film structures in nanoindentation configuration [4–7]. These measurements rely on the interdependence of the force applied to the tip and the indentation depth created during nanoindentation. The measured force–distance curve is used to calculate the hardness and Young's modulus [8]. In this work, we will discuss the impact of growth conditions on the hardness and Young's modulus of zirconium carbonitride based spectrally selective coatings. The observed mechanical properties are strongly related to the zirconium nitride fraction in ZrC–ZrN matrix of the tandem absorber structures. The studies suggest that optimal nitrogen flow rate is important to achieve the enhanced solar thermal performance, which corresponds to the moderate mechanical properties. The lower and higher values of hardness and Young's modulus lead to the poor solar thermal performance and may not be useful for field applications.

2 Experimental Details

The synthesis of ZrO_x/ZrC–ZrN/Zr spectrally selective reflector–absorber tandem structures has been described by Usmani et al. in detail elsewhere [1]. In brief, ZrO_x/ZrC–ZrN/Zr structures are deposited on stainless steel, SS, and aluminum, Al, substrates using DC/RF magnetron sputtering in three sequential steps. First, DC magnetron sputtering was used to deposit Zr metallic reflector, followed by reactive RF magnetron sputtering for ZrC–ZrN absorber layer. Finally, ZrO_x layer was deposited using reactive DC magnetron sputtering. The details about their structural, microstructural, optical, and thermal properties are discussed in Ref. [1]. Mechanical properties of ZrO_x/ZrC–ZrN/Zr structures on both SS and Al substrates are investigated using nanoindentation technique. The nanoindenter, used for mechanical measurements, is an integrated accessory with atomic force microscopy (scanning probe microscopy (SPM) XE-70, Park) system. AFM was operated in contact mode for these mechanical properties measurements over 5×5 μm^2 scan areas. The Berkovich indenter, a sapphire cantilever with a diamond tip, has been used for indentation on ZrO_x/ZrC–ZrN/Zr/Substrates top surface. This indenter was initially forced into the ZrO_x/ZrC–ZrN/Zr surface at constant load with the forward (down) speed of about 0.3 μm/s and was kept for 10 s at that depth, followed by unloading at a backward (up) speed of about 0.3 μm/s. Ten such indentations were carried out on each sample at different physical locations, to measure the average hardness and Young's modulus using the generated load–displacement curves. The measured load versus displacement graphs were used to calculate stiffness S (=dP/dh) by estimating the slope of the upper portion of the unloading curve. The calculated stiffness S and projected contact area of the indented tip A were used to estimate the effective Young's modulus of these multilayer structures using the following equation [9]:

$$\frac{1}{E_{\text{eff}}} = \frac{2\beta}{S}\sqrt{\frac{A}{\pi}} = \frac{1 - v_s^2}{E_s} + \frac{1 - v_i^2}{E_i},$$

where E_{eff} is the effective modulii for each indenter/specimen combination, and β is a shape constant of 1.034 for the Berkovich tip [4]. E and v represent the Young's modulus and Poison's ratio of the indenter, i, and the sample, s, respectively. The values, used for Poisson's ratio v and Young's modulus E_i for diamond indenters, are 0.07 and 1141 GPa [10]. The Poisson's ratio for samples used is $\sim$0.3 [11]. Simultaneously, the hardness values are calculated using $H = \frac{P_{\max}}{A}$, where $P_{\max}$ is the maximum load in a load–displacement curve.

3 Results and Discussion

Sputter deposition parameters are important to optimize for the optimal solar thermal response of spectrally selective absorbers in the desired wavelength range. In our previous work, we have discussed the optimization of spectrally selective ZrO_x/ZrC–ZrN/Zr reflector–absorber tandem structures, by varying nitrogen flow rate for the absorber layer during deposition [1, 2]. The maximum absorptivity $\alpha \sim 0.9$ and the minimum emissivity $\varepsilon \sim 0.04$ have been observed for 12.5 sccm nitrogen flow during ZrC–ZrN layer deposition. ZrN phase fraction was increasing with an initial increase in nitrogen flow rate initially and exhibited maxima at 12.5 sccm, followed by a decrease with any further increase for both SS and Al substrates [1]. The ZrN phase fraction has been calculated using X-ray diffraction

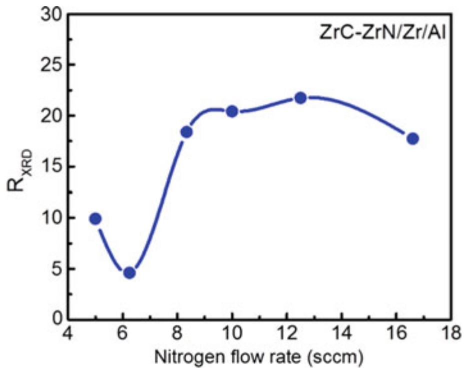

Fig. 1 Zirconium nitride (ZrN) phase fraction in zirconium carbide and zirconium nitride (ZrC–ZrN) matrix as a function of nitrogen flow rate, used during synthesis of the ZrC–ZrN absorber layer

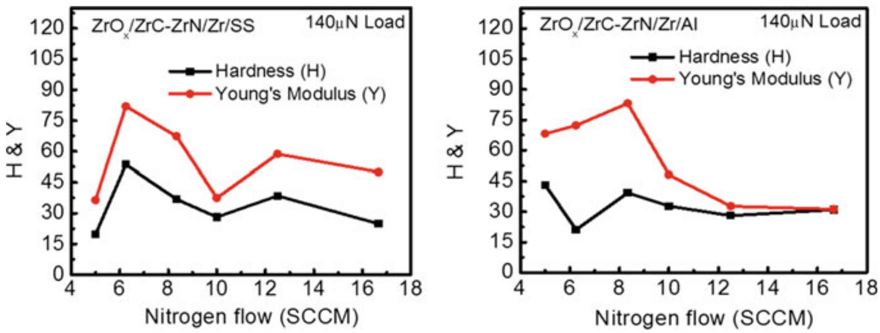

Fig. 2 *Left panel* Hardness (H) and Young's modulus (Y) of ZrO_x/ZrC–ZrN/Zr tandem absorber film on SS substrate and *right panel* on Al substrate

measurements of ZrC–ZrN absorber layer in ZrO_x/ZrC–ZrN/Zr structure on Al substrate. The measured relative ZrN phase fraction in ZrC–ZrN absorber matrix has been shown in Fig. 1, as a function of nitrogen flow rate. This variation in ZrN phase fraction suggests that the maximum is near ~10–12.5 sccm nitrogen flow rate, used for the synthesis of ZrC–ZrN absorber layer.

The mechanical properties are important and assist in understanding the materials strength and durability. The nanoindentation measurements have been carried out to calculate the hardness and Young's modulus of ZrO_x/ZrC–ZrN/Zr structures. The nanoindentation depth ~50 nm is much smaller as compared to the thickness of the entire ZrO_x/ZrC–ZrN/Zr structure ~600 nm. The thickness of ZrO_x/ZrC–ZrN/Zr structure is sufficient to exclude the substrate effect on these measured mechanical properties and thus, the measured values can be considered mostly from the ZrOx/ZrC–ZrN/Zr structures only. The measured values of hardness and Young's modulus are summarized in Fig. 2 for both SS (left panel) and Al (right panel) substrates, as a function of nitrogen flow used for the synthesis of ZrC–ZrN absorber layer. The hardness values show strong variation for ZrO_x/ZrC–ZrN/Zr structures, with lower nitrogen flow rates, used for ZrC–ZrN layer and approached nearly constant value at 10 or higher sccm nitrogen flow rates, for both SS and Al substrates. The hardness values are prone to the film properties such as films' density, microstructure, and surface roughness [12]. Thus, samples with 10 sccm or higher nitrogen flow may be showing less surface roughness with optimal density of ZrC–ZrN composite absorber, causing nearly constant hardness values in contrast to lower nitrogen flow rates, where effective density of ZrC–ZrN may be lower and also surface properties may be poor, leading to large variation in hardness values. The maximum selectivity of ZrO_x/ZrC–ZrN/Zr tandem structure selective absorber was found around 12.5 sccm nitrogen flow rate used for ZrC–ZrN absorber layer [1], suggesting moderate values of hardness may be relatively better for solar thermal performance.

The elastic modulus is a measure of the stiffness of the material and Young's modulus has been used to understand stiffness properties. Young's modulus also exhibits the similar trend like hardness values, which nearly saturates toward higher nitrogen flow rates, in conjunction with initial large fluctuations. The reason of such fluctuation is not clear for samples deposited at lower nitrogen flow rates. Hardness and Young's modulus values of ZrO_2, ZrN, and ZrC single-layer thin film are 13.5–19 GPa, 13.4–23.5 GPa, 27.6 GPa and 197–210 GPa, 166.4–196.3 GPa, 228 GPa, respectively [12–14]. Interestingly ZrO_x/ZrC–ZrN/Zr tandem structures exhibit higher values of hardness as compared to that of ZrO_2, ZrN, and ZrC single-layer thin film hardness values. However, Young's modulus values show contrary behavior with relatively smaller values as compared to ZrO_2, ZrN, and ZrC single-layer thin film values. This is possible as hardness and Young's modulus in the present work is the effective values of multilayer ZrO_x/ZrC–ZrN/Zr structures in contrast to the single layer independently.

Further, we carried out load versus displacement curves at different initial load conditions on the sample with the optimal solar thermal properties $\alpha \sim 0.9$ and $\varepsilon \sim 0.04$, synthesized suing 12.5 sccm nitrogen flow rate to understand the impact of external load on mechanical properties. The measured different loads versus displacement curves are shown in Fig. 3a–e, which are used to measure the hardness and Young's modulus values at these initial load conditions. The respective insets show the microscopic image of the indented area, created during nanoindentation measurements.

These nanoindentation profiles suggest that depth of such indentations increases with increasing load, as noticed with increased diameter and marked in insets for clarity. The measured H and Y values as a function of load are summarized in Fig. 3f for this sample within the elastic limit. These measured values suggest that initially both hardness and Young's modulus values are increasing with load up to ~ 140 μN and reached to nearly constant hardness and Young's modulus values, independent of load conditions.

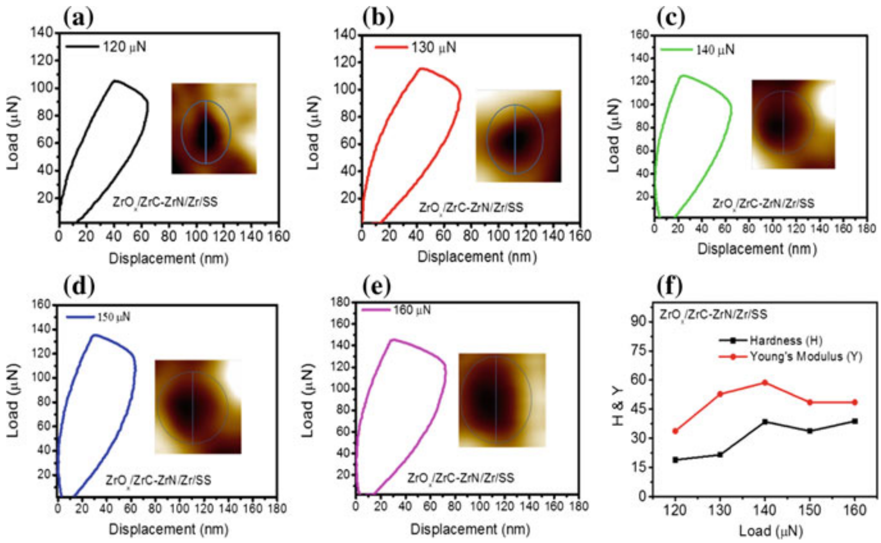

Fig. 3 The load versus displacement curve at difference end loads, **a**–**e** with inset showing the respective AFM indentation profiles and hardness and Young's modulus values versus load, **f** for ZrO_x/ZrC–ZrN/Zr tandem structure with ZrC–ZrN absorber layer synthesizes at 12.5 sccm nitrogen flow

4 Conclusion

ZrO_x/ZrC–ZrN/Zr reflector–absorber tandem spectrally selective surfaces were deposited on stainless steel (SS) and aluminum (Al) substrates, using RF/DC sputtering system with varying nitrogen flow rate during ZrC–ZrN absorber layer deposition. AFM nanoindentation method has been used to understand the mechanical properties of ZrO_x/ZrC–ZrN/Zr structures on both substrates. The hardness and Young's modulus values increase from ~19.63 to ~38.53 GPa and ~36.39 to ~58.67 GPa with increasing nitrogen flow rate of the absorber layer. These mechanical properties also exhibit an increasing trend with varying load up to 140 μN, which becomes constant with any further load increase. These studies suggest that absorber growth conditions have a strong influence on mechanical properties and moderate hardness and Young's modulus values may be important with optimal solar thermal performance.

Acknowledgements Authors gratefully acknowledge the financial assistance, from the Ministry of New and Renewable Energy (MNRE), India through grant 15/40/2010-11/ST, to carry out experimental work.

References

1. B. Usmani, A. Dixit, Spectrally selective response of ZrO_x/ZrC–ZrN/Zr absorber-reflector tandem structures on stainless steel and copper substrates for high temperature solar thermal applications. Sol. Energy **134**, 353–365 (2016)
2. B. Usmani, A. Dixit, Impact of corrosion on microstructure and mechanical properties of ZrO_x/ZrC–ZrN/Zr absorber-reflector tandem solar selective structures. Sol. Energy Mater. Sol. Cells **157**, 733–741 (Accepted, 2016)
3. B. Usmani, V. Vijay, R. Chhibber, L. Chandra, A. Dixit, Zirconium car bide-nitride composite matrix based solar absorber structures on glass and aluminum substrates for solar thermal applications, in ISES Solar World Congress 2015 Proceeding (in press)
4. T.-H. Fang, S.-R. Jian, D.-S. Chuu, Nanomechanical properties of TiC, TiN and TiCN thin films using scanning probe microscopy and nanoindentation. Appl. Surf. Sci. **228**, 365–372 (2004). https://dx.doi.org/10.1016/j.apsusc.2004.01.053
5. S.A. Catledge, J. Borham, Y.K. Vohra, W.R. Lacefield, J.E. Lemons, Nanoindentation hardness and adhesion investigations of vapor deposited nanostructured diamond films. J. Appl. Phys. **91**, 5347 (2002). https://dx.doi.org/10.1063/1.1464233
6. R. Navamathavan, D. Arivuoli, G. Attolini, C. Pelosi, Nanoindentation studies of (111) GaAs/InP epilayers. Appl. Surf. Sci. **180**, 119–125 (2001). https://dx.doi.org/10.1016/S0169-4332(01)00336-1
7. N.R. Moody, W.W. Gerberich, N. Burnham, S.P. Baker, *Fundamentals of Nanoindentation and Nanotribology* (Materials Research Society, Warrendale, PA, 1998)
8. R. Ferencz, J. Sanchez, B. Blumich, W. Herrmann, AFM nanoindenta tion to determine Young's modulus for different EPDM elasto mers. Polym. Test. **31**, 425–432 (2012). https://dx.doi.org/10.1016/j.polymertesting.2012.01.003
9. W.C. Oliver, G.M. Pharr, Measurement of hardness and elastic modulus by instrumented indentation advances in understanding and refinements to the methodology. Mater. Res. Soc. **19**, 3–20 (2004). https://dx.doi.org/10.1557/jmr.2004.19.1.3
10. W.C. Oliver, G.M. Pharr, An improved technique for determining hardness and elastic modulus using load and displacement sensing indentation experiments. J. Mater. Res. (1992). https://dx.doi.org/10.1557/JMR.1992.1564
11. J.F. Shackelford, W. Alexander, Materials Science and Engineering Handbook, 3rd edn. (CRC Press LLC, 2001)
12. C.S. Chen, C.P. Liu, C.Y.A. Tsao, H.G. Yang, Study of mechanical properties of PVD ZrN films, deposited under positive and negative substrate bias conditions. Scr. Mater. **51**, 715–719 (2004). https://dx.doi.org/10.1016/j.scriptamat.2004.06.005
13. D. Craciun, G. Socol, G. Dorcioman, N. Stefan, G. Bourne, V. Craciun, High-quality ZrC, ZrC/ZrN and ZrC/TiN thin films grown by pulsed laser deposition. J. Optoelectron. Adv. Mater. **12**, 461–465 (2010)
14. Z.W. Zhao, W. Lei, X.B. Zhang, B.P. Wang, B.K. Tay, Nanocrystalline zirconium oxide thin films grown under low pulsed dc voltages. J. Phys. D Appl. Phys. **42**, 215408 (2009). https://dx.doi.org/10.1088/0022-3727/42/21/215408